BJET
(Bayero Journal of Engineering and Technology)
https://bjet.ng/index.php/jet

Research Article
2025, Vol. 20 (1), 81-95

OPTIMISATION OF BIODIESEL PRODUCTION FROM MAHOGANY SEED OIL USING CALCINED BANANA PEEL CATALYST VIA RESPONSE SURFACE METHODOLOGY

D. Baba[1,2*], U.O. Aroke [2], J. Mohammed[2], and S.O. Giwa[2]

[1] Department of Chemical Engineering, Faculty of Engineering, University of Maiduguri, Maiduguri, Borno State, Nigeria.

[2*] Department of Chemical Engineering, Faculty of Engineering and Engineering Technology, Abubakar Tafawa University, Bauchi, Nigeria.

Email: dbaba@unimaid.edu.ng

Received: 07-06-2025
Revised: 17-06-2025
Accepted: 12-07-2025
Published: 16-07-2025

Abstract: This study explores the feasibility of using calcined banana peel (CBP) as a heterogeneous catalyst for biodiesel production from non-edible mahogany seed oil (MSO). The research addresses sustainability and cost concerns of conventional biodiesel production while mitigating ethical issues associated with edible oil feedstocks and environmental impacts of traditional catalysts. The CBP catalyst was prepared and comprehensively characterised using FTIR, SEM-EDS, and BET surface area analysis, revealing a surface area of 527.6 m^2/g with a pore volume of 0.264 cm^3/g. The transesterification process was optimised using response surface methodology (RSM) with a central composite rotatable design (CCRD) to determine the effects of reaction time, temperature, methanol-to-oil molar ratio, and catalyst concentration on biodiesel yield. Optimum conditions were determined to be a reaction time of 156 minutes, a temperature of 66°C, and a catalyst concentration of 2.45%. Under these conditions, the maximum experimental biodiesel yield was 59.61%, which compared well with the predicted value of 61.65%. GC-MS analysis confirmed the biodiesel's composition as primarily fatty acid methyl esters (FAMEs), with methyl oleate and methyl linoleate as major components. Analysis of key physicochemical properties demonstrated that the mahogany biodiesel largely meets ASTM standards for fuel quality. These findings demonstrate the potential of CBP as a viable and sustainable heterogeneous catalyst for efficient MSO biodiesel production, offering a promising route to reduce waste, utilise non-edible feedstocks, and enhance biofuel industry sustainability.

Key words: Biodiesel, Heterogeneous catalysts, Mahogany seed oil, Optimization, Response Surface Methodology, Transesterification

1 Introduction

The increasing global demand for sustainable and renewable energy is driving intensified research into biodiesel production, a clean-burning alternative to petroleum diesel. Derived from renewable biological sources such as vegetable oils and animal fats, biodiesel offers a promising route to mitigate environmental concerns and reduce reliance on fossil fuels (Mathew et al., 2021). Biodiesel presents numerous advantages over fossil diesel, including reduced greenhouse gas emissions, particulate matter, sulfur oxides, and carbon monoxide, alongside improved cetane number, lubricity, and biodegradability (Hassan et al., 2022; Pydimalla et al., 2023). However, significant challenges persist, notably high production costs, limited oxidative stability, and poor cold flow properties.

A key factor in addressing the sustainability and economic viability of biodiesel is feedstock selection. Diverse options exist, each with trade-offs. Edible oils like soybean, rapeseed (canola), sunflower, and palm oil boast high oil content and well-established production systems, leading to efficient biodiesel yields (Hemavathy et al., 2024; Kumar et al., 2025). Their low free fatty acid (FFA) content simplifies processing. However, utilizing edible oils for fuel raises ethical "food vs. fuel" concerns, potentially impacting food security and prices (Elgharbawy et al., 2021). Furthermore, expansion of edible oilseed cultivation can contribute to deforestation and land use change

(Vijay et al., 2018), and these oils are often more expensive, affecting biodiesel's economic competitiveness (Elgharbawy et al., 2021).

Non-edible oils, including jatropha, neem, karanja, mahua, and mahogany, offer a sustainable alternative by avoiding competition with food sources and promoting food security. These feedstocks can be cultivated on marginal lands, supporting sustainable land use practices (Vijay et al., 2018), while their lower costs enhance economic viability. However, challenges include higher FFA content that often necessitates pre-treatment (Takase & Essandoh, 2021; Zhou et al., 2021), potential impurities requiring removal (Takase & Essandoh, 2021), and less developed production systems that may hinder scale-up. Waste cooking oil (WCO) represents another eco-friendly feedstock, reducing waste and offering low-cost input (Hemavathy et al., 2024; Pydimalla et al., 2023), though quality variability demands stringent control and pre-treatment (Hemavathy et al., 2024). Microalgae and animal fats are also explored, facing challenges in large-scale cultivation, lipid extraction (Yin et al., 2020), and sustainability concerns (Gebremariam & Marchetti, 2018).

Among the diverse non-edible oil feedstocks, mahogany (Khaya senegalensis) seed oil stands out as a particularly promising candidate for sustainable biodiesel production (Salih & Yahia, 2015). The Khaya senegalensis tree, abundant across Africa, yields seed often discarded as waste. These seeds contain a significant oil content of 52.5% (Soja et al., 2017), offering a valuable resource for biofuel production within a circular economy framework. Utilizing mahogany seeds transforms waste into valuable resources, ensuring a consistent, renewable supply. Furthermore, its favourable fatty acid profile, comparable to established vegetable oils (Soja et al., 2017), underscores mahogany seed oil's potential as a viable and environmentally sound biodiesel feedstock.

Mahogany seed oil biodiesel production relies on transesterification, converting triglycerides to fatty acid methyl esters (FAME) and glycerol using methanol and a catalyst. While homogeneous catalysts, such as sodium hydroxide (NaOH) and potassium hydroxide (KOH), offer high activity and are cost-effective, they present significant drawbacks, including corrosion, soap formation, difficult separation, and wastewater generation, hindering their long-term sustainability. Heterogeneous catalysts, in contrast, offer easier separation, reusability, and reduced environmental impact. However, they often exhibit lower activity and mass transfer limitations compared to their homogeneous counterparts.

To overcome these limitations of both homogeneous and traditional heterogeneous catalysts, this study explores a novel approach: the utilization of calcined banana peel as a heterogeneous catalyst. Banana peel, an abundant agricultural waste, presents a cost-effective and environmentally benign alternative. Rich in alkaline earth metal oxides, particularly potassium oxide (K_2O), magnesium, and calcium (Gupta et al., 2025), calcination transforms banana peels into porous carbon structures with these active metal oxides (Meriatna et al., 2023). Calcined banana peel has demonstrated effectiveness in biodiesel production from various feedstocks, showcasing its catalytic potential (Boyle et al., 2025; Tarigan et al., 2023). This approach not only valorises waste but also offers a sustainable alternative to conventional catalysts.

Given the promising catalytic properties of calcined banana peel, optimizing its application for mahogany seed oil transesterification becomes crucial for maximizing biodiesel yield. To achieve this optimization, response surface methodology (RSM) was employed as a systematic approach to determine the optimal operating conditions. While banana peel has shown promise as a catalyst in other biodiesel systems, its efficacy and optimal application for mahogany seed oil transesterification, particularly using RSM for optimization, remains unexplored. This research addresses this knowledge gap by systematically investigating and optimizing the transesterification process using calcined banana peel as a catalyst. By varying factors such as catalyst loading, methanol-to-oil ratio, reaction temperature, and reaction time, RSM enables the identification of optimal conditions for maximizing biodiesel production.

This research aims to demonstrate the efficacy of calcined banana peel as a sustainable catalyst for mahogany seed oil biodiesel production and to optimize the transesterification process for high-quality biodiesel output. This investigation holds the potential to significantly contribute to sustainable biodiesel production by enabling the valorisation of agricultural waste and the efficient utilization of non-edible oil feedstocks, paving the way for more environmentally sound and economically viable biofuel industries.

2 Methodology

2.1 Catalyst Preparation and Characterization

Calcined banana peel catalyst was prepared following the method of Tarigan et al. (2023). The fresh banana peels were thoroughly washed with distilled water to remove surface impurities. The peels were initially dried in an oven at 60 °C for 24 h to partially remove moisture, followed by sun-drying for four days until the peels became brittle and reached a constant weight.

The dried peels were then ground using a laboratory blade grinder (SHB-3088 YR05264 by Kalstein) and sieved through a 1 mm mesh to obtain a uniform particle size (Figure 1 (a)). The sieved powder was further dried in an oven at 100 °C for 2 h to ensure complete removal of any reabsorbed moisture before calcination. Calcination was performed in a muffle furnace under an air atmosphere at 600 °C for 6 h, with a gradual temperature ramp at a rate of 5 °C/min to prevent thermal shock. After calcination, the muffle furnace was allowed to cool naturally to room temperature with the door closed before the catalyst was removed (Figure 1 (b)). Finally, the catalyst was weighed using an analytical balance. The prepared catalyst was characterized using Fourier-transform infrared spectroscopy (FTIR), X-ray photoelectron spectroscopy (XPS), Brunauer-Emmett-Teller (BET) surface area analysis, and Scanning Electron Microscopy (SEM).

(a) (b)

Figure 1*: Banana peel powder (a) before calcination (b) after calcination*

2.2 Experimental Design

Central composite rotatable design (CCRD), known for its effectiveness in response surface methodology (RSM) and its rotatability (with α = 1 for this face-centred design), was employed as the experimental design. Given the complex and heterogeneous nature of banana peel-derived catalysts, it was hypothesised that the transesterification process may exhibit non-linear relationships between reaction parameters and biodiesel yield. CCRD is well-suited to capture these complex relationships and identify optimal operating conditions by exploring a broader range of conditions than simpler factorial designs. This design is particularly advantageous due to its efficiency in fitting quadratic response surfaces and accurately predicting optimal conditions, making CCRD ideal for this study aiming to maximize biodiesel production using a banana peel catalyst.

Table 1 summarizes the key independent variables investigated in this study using the central composite rotatable design (CCRD) that influences the transesterification reaction and biodiesel yield. The table presents the actual experimental values corresponding to the coded levels used in the CCRD matrix.

Table 1: Independent Variables and Levels Used for Central Composite Rotatable Design (CCRD)

Independent Variable	Symbol	Lower Level (-α)	Upper Level (+α)
Reaction Time (min)	A	30	120
Reaction Temperature (°C)	B	40	70
Methanol-Oil Ratio	C	4:1	12:1
Catalyst Concentration (wt%)	D	1	5

The primary response variable was biodiesel yield, defined as the percentage of fatty acid methyl esters (FAMEs) produced relative to the initial weight of the mahogany seed oil (MSO). It was calculated by dividing the weight of the produced biodiesel (FAMEs fraction) by the weight of the starting MSO, multiplied by 100 (Madai et al., 2020). The complete formula for biodiesel yield calculation is provided in Equation 1.

$$\text{Biodiesel yield (\%)} = \frac{\text{Weight of biodiesel produced}}{\text{Weight of mahogany oil used}} \times 100\% \quad \ldots (1)$$

2.3 Transesterification Procedure

Transesterification reactions were conducted in a 250 mL round-bottom flask fitted with a magnetic stir bar, a Liebig reflux condenser (Figure 2) using cooling water from a chiller as coolant, and a heating mantle with digital temperature control. For each reaction run, calcined banana peel catalyst was mixed with 100 mL of anhydrous methanol (99.9% purity) in a separate 250 mL beaker and stirred for 5 min to ensure proper

dispersion. 10 mL of MSO was accurately measured and preheated to 40oC using the heating mantle for 5 min to reach the desired starting temperature. The pre-mixed methanol-catalyst slurry was then rapidly added to the preheated MSO in the reactor. The transesterification reaction was then carried out under the specific conditions of reaction temperature and reaction time as determined by the Central Composite Rotatable Design (CCRD). Throughout the reaction, the mixture was continuously stirred at 300 rpm. After the reaction time specified by the CCRD was complete, the reaction mixture was immediately removed from the heating mantle and allowed to cool slightly. The catalyst was then separated from the reaction mixture by hot gravity filtration using Whatman No. 1 filter paper (pore size 11 µm) in a heated filtration funnel to ensure efficient removal of solid catalyst particles and prevent solidification of reaction products.

***Figure 2**: Experimental Set-up for the Mahogany Seed Oil Transesterification*

2.4 Separation and Product Collection

The filtrate (containing biodiesel, glycerol, unreacted methanol, and unreacted oil) was transferred to a separating funnel and allowed to settle at room temperature for 12 hours. After settling for 12 hours, the lower glycerol layer was carefully drained off from the bottom of the separating funnel, and the upper biodiesel layer was then collected, weighed, and stored in airtight containers.

2.5 Biodiesel Physicochemical Properties

The following properties were determined according to standard methods:

Acid Value and FFA Content

Acid values of the sample were determined according to ASTM D-974-00 (ASTM International, 2018). 0.5 g of sample was weighed into 250 ml conical flask. 50 ml of neutralized ethyl alcohol was added. The mixture was heated on a water bath to dissolve the sample. The solution was titrated against 0.1 M KOH using phenolphthalein as an indicator. The acid value was determined, after which the free fatty acid was calculated as shown in Equations 2 and 3.

$$\text{Acid Value (mg KOH/g)} = \frac{(V * N * 56.1)}{W} \quad \ldots (2)$$

Where: V = Volume of KOH titrant (mL), N = Normality of KOH solution, W = Weight of biodiesel sample (g), 56.1 = Molecular weight of KOH (g/mol).

$$\text{FFA Content (\%)} = \frac{Acid\ Value \times 282}{56.1} \quad \ldots (3)$$

Where: Acid Value is the value obtained from Equation 2, 282 = Molecular weight of oleic acid (g/mol), 56.1 = Conversion factor (mg KOH per mEq).

Peroxide Value

This is the measure of its content of oxygen. It is expressed in mol/kg. 2 g of the sample and 1g of powdered potassium iodide was added into 2 test tubes containing 20 ml of solvent mixture each (2 vol. glacial acetic acid + 1 vol. of chloroform) i.e. (60:30). Step 1 was carried out in a blank tube (without sample). The tubes were placed in a water bath and allowed to boil vigorously for 30 seconds. The contents were poured quickly into a conical flask containing 10 ml of 5% potassium iodide solution. The tubes were washed with 5 ml of water each and poured into each conical flask with contents, and 4 drops of phenolphthalein were then added into each conical flask and were titrated with 0.01M thiosulfate until a colour change was obtained (AOCS, 2017).

$$Peroxide\ Value\ (meq\ O2/kg\ biodiesel) = \frac{(S-B)\times N \times 1000}{W} \quad \ldots (4)$$

Where: S = Volume of sodium thiosulphate titrant for sample (mL), B = Volume of sodium thiosulphate titrant for blank (mL), N = Normality of sodium thiosulphate solution, W = Weight of biodiesel sample (g).

Refractive Index

Abbey Refractometer was used in this determination according to A. I. ASTM (2021). A drop of the sample was transferred into a glass slide of the refractometer.

Water at 30 oC was circulated through the glass slide to keep its temperature uniform. Through the eyepiece of the refractometer, the dark portion viewed was adjusted to be in line with the intersection of the cross. At no parallax error, the pointer on the scale pointed to the refractive index. This was repeated, and the mean value noted and recorded as the refractive index.

Density

The densities of the sample were determined according to the ASTM D1298-12b standard test method (I. ASTM, 2018). The sample was brought to a specified temperature, and a test portion was transferred to a hydrometer cylinder that had been brought to approximately the same temperature. The appropriate hydrometer, also at a similar temperature, was lowered into the test portion and allowed to settle. After temperature equilibrium had been reached, the hydrometer scale reading and the temperature of the test portion were taken. The observed hydrometer reading was reduced to the reference temperature by means of a petroleum measurement table. Any hydrometer correction was applied to the observed reading, and the corrected hydrometer scale reading was recorded to the nearest 0.1kg/m3 as density.

Dynamic Viscosity

The viscosity of the oil was determined using Brookfield Digital rotational viscometer (NDJ-8S) according to ASTM D- 445. The sample was heated in the hot oil bath, and the spindle of the viscometer was fitted into the melted wax. The speed was selected, and the start button was pressed for the spindle to rotate and give the angle of rotation, including the viscosity measurement and operating temperature on the display (I. ASTM, 2018).

$$\text{Kinematic viscosity (cSt)} = \frac{\text{Dynamic viscosity (mPa·s)}}{\textit{Density}\ \text{(g/cm3)}} \quad \ldots (5)$$

Cloud and Pour Points

Cloud and Pour Points were determined using a Cloud/Pour Point tester according to ASTM D2500 (I. ASTM, 2018).

Flash and Fire Points

Flash and Fire Points were determined using a flash point tester with visual observation of ignition following ASTM D93 (ASTM, 2018) for flash point and ASTM D92 (ASTM, 2018) for fire point determination.

Cetane Number

Cetane Number is measured using an Octane/Cetane meter in accordance with ASTM D613 (ASTM International, 2018) for the automated method.

Heating Value

Heating Value (Calorific Value) was determined using a Bomb Calorimeter (Model 6100, Parr Instrument Co.) according to ASTM D2382-88 (ASTM, 2008).

3 Results and Discussion

This section presents and discusses the key results obtained in this study. We first analyse the experimental data from the Central Composite Rotatable Design (CCRD) to statistically model and optimize biodiesel production. Subsequently, the characterization of the banana peel catalyst and the physicochemical properties of the produced biodiesel was presented.

3.1 Statistical Analysis of Mahogany Seed Oil Biodiesel Production

The experimental data generated from the CCRD was subjected to response surface methodology (RSM) using Design-Expert software. This analysis aimed to statistically model the transesterification process, evaluate the individual and interactive effects of reaction time, temperature, methanol-oil molar ratio, and catalyst concentration on biodiesel yield, and ultimately, to identify optimal conditions for maximizing biodiesel production. Table 2 presents the complete CCRD experimental matrix, detailing the specific combinations of independent variables (reaction time, temperature, methanol-oil molar ratio, and catalyst concentration) used in each run, along with the corresponding biodiesel yields obtained. From this experimental dataset, the maximum observed biodiesel yield was 60.2%, achieved in Run 25, under the following conditions: reaction time of 98 min, reaction temperature of 63°C, a methanol-to-oil molar ratio of 10:1, and a catalyst concentration of 2 wt%.

Table 2: *CCRD Experimental Matrix and Biodiesel Yield*

Time (A) min	Temp. (B) (°C)	MOH/OIL (C)	at. Conc.)) (wt%)	Biodiesel yield
53	48	10:1	2	45.9
75	40	8:1	3	36.8
75	55	4:1	3	20.1
75	55	8:1	3	30.7
53	63	6:1	4	44.0
98	48	10:1	2	50.1
53	63	6:1	2	20.2
75	55	12:1	3	48.2
98	48	6:1	2	17.8

75	70	8:1	3	23.4
75	55	8:1	3	34.1
98	63	6:1	2	43.5
53	48	6:1	4	41.2
120	55	8:1	3	22.0
75	55	8:1	3	37.6
53	48	6:1	2	10.5
98	63	6:1	4	50.5
98	63	10:1	4	25.2
53	63	10:1	4	14.0
53	63	10:1	2	17.5
75	55	8:1	5	38.7
75	55	8:1	3	21.3
75	55	8:1	1	38.9
98	48	6:1	4	20.8
98	63	10:1	2	60.2
98	48	10:1	4	20.4
53	48	10:1	4	54.1
75	55	8:1	3	37.1
30	55	8:1	3	25.9
75	55	8:1	3	40.0

3.2 Model Adequacy and Statistical Significance

The analysis of variance (ANOVA) for the quadratic model of biodiesel yield (Table 3) revealed a statistically significant model (F value = 12.00, $p < 0.0001$), indicating that the model is a significant predictor of biodiesel yield from mahogany seed oil using a calcined banana peel catalyst. Furthermore, the non-significant lack of fit ($p = 0.587$) indicates that the quadratic model adequately captures the relationships between the independent variables and biodiesel yield within the experimental range studied. Similar observations have been reported by Eze et al. (2025), where the lack of fit was non-significant (0.203), supporting the model's adequacy in describing biodiesel production systems.

Among the individual factors, the methanol-to-oil ratio (C) was identified as having a statistically significant effect on biodiesel yield ($p = 0.0044$), consistent with literature emphasizing the methanol-to-oil ratio as a critical parameter influencing transesterification efficiency (Degfie et al., 2019). Notably, reaction time (A), temperature (B), and catalyst concentration (D) did not show significant linear effects when considered individually, which has also been observed in other studies where these factors exhibited significance primarily through interaction effects rather than as sole linear terms (Eze et al., 2025).

ANOVA highlighted the critical role of interaction effects. Highly significant two-factor interactions were observed between reaction time and temperature (AB, $p < 0.0001$), reaction time and catalyst concentration (AD, $p = 0.0003$), temperature and methanol-to-oil ratio (BC, $p = 0.0001$), and methanol-to-oil ratio and catalyst concentration (CD, $p = 0.0001$). These significant interactions underscore the complex and interdependent nature of these process variables and their combined influence on biodiesel yield, emphasizing the need for simultaneous optimization. Degfie et al. (2019) similarly demonstrated the importance of interaction effects in biodiesel yield optimization, highlighting the nonlinear and synergistic relationships among process parameters.

Table 3: *Analysis of Variance for the Transesterification Model*

Source	Sum of Square	df	F-val	p-value	
Model	4178.58	8	12.0	< 0.0001	significant
A-Time	25.85	1	0.59	0.4494	
B-Temp.	9.18	1	0.21	0.6507	
C-	443.28	1	10.1	0.0044	
D-Cat.	1.83	1	0.04	0.8395	
AB	1023.26	1	23.5	< 0.0001	
AD	810.13	1	18.6	0.0003	
BC	946.21	1	21.7	0.0001	
CD	968.77	1	22.2	0.0001	
Residual	913.96	21			
Lack of	684.90	16	0.93	0.5870	not sig.
Pure	229.05	5			
Cor Total	5092.53	29			
Std. Dev.	6.60		R^2		0.8205
Mean	33.02		Adjusted R^2		0.7522
C.V. %	19.98		Predicted R^2		0.6453
			Adeq Precision		11.4578

This complex relationship is quantitatively described by the fitted quadratic regression equation (Equation 6):

$$Yield\ (\%) = -178.562 - 1.609A + 0.465B + 42C + 55.118D + 0.047AB - 0.316AD - 0.512BC - 3.891CD. \quad \ldots (6)$$

The model showed a good fit to the experimental data as evidenced by an R^2 value of 0.8205 and an adjusted R^2 of 0.7522. The predicted R^2 of 0.6453, while slightly lower, still suggests reasonable predictive ability. An Adequate Precision value of 11.4578, which exceeds the desirable threshold of 4, indicates an adequate signal-to-noise ratio for navigating the design space with this model. These model fit statistics are comparable to those reported in related biodiesel optimization studies (Degfie et al., 2019; Eze et al., 2025).

3.3 Model Adequacy Check

To validate the assumptions underlying the quadratic model, we carefully examined diagnostic plots. The Predicted vs. Actual yield plot (Figure 3) demonstrated a good level of agreement between predicted and observed biodiesel yields, indicating the model effectively captured the primary trends within the experimental data. While most data points clustered closely around the line of perfect prediction, suggesting strong model performance, some divergences were noted. For instance, run 7 exhibited a significantly higher actual yield than its predicted value. Such discrepancies could stem from uncaptured interaction effects or other unaccounted variables influencing the reaction.

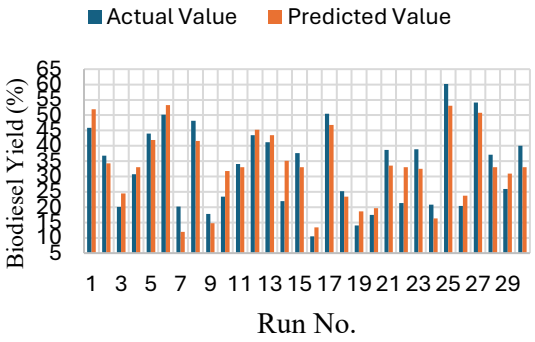

Figure 3: *Actual and Predicted Mahogany Seed Oil Biodiesel Yield for the Various Run.*

Further assessment using the Normal Probability Plot of Residuals (Figure 4a) revealed that the residuals approximately followed a straight line, indicating reasonable adherence to the normality assumption.

This finding aligns with standard practices in regression diagnostics, where normality of residuals supports the validity of statistical inference in response surface methodology (RSM) models (Jensen, 2014).

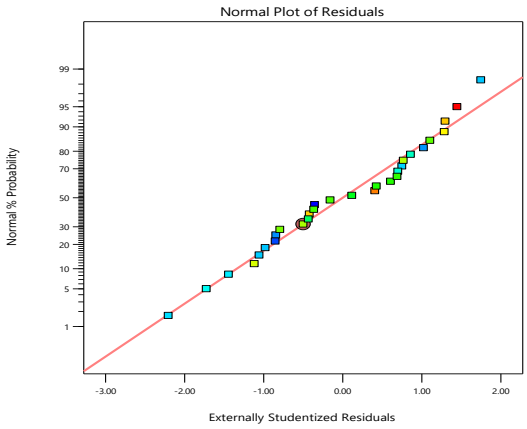

(a)

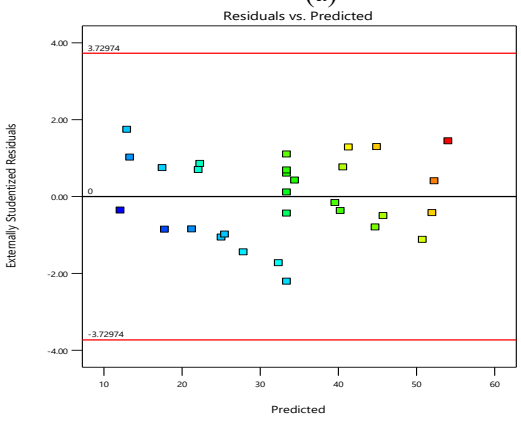

(b)

Figure 4: *Diagnostic Plots of Mahogany Seed Oil Biodiesel (a) Normal Plot of Residuals and (b) Residuals Plot*

The Residuals vs. Predicted plot (Figure 4b) displayed a random scatter of residuals with no discernible patterns and roughly constant variance across the predicted yield range, supporting the assumption of constant variance and randomness of errors (Montgomery & Cahyono, 2022).

Despite the inherent variability common in experimental biodiesel data and the simplifications intrinsic to statistical modelling, these diagnostic checks affirm the adequacy and validity of the quadratic model in capturing the biodiesel transesterification process within the experimental design space investigated. Such validation enhances confidence in the model's predictive capability and underpins the reliability of subsequent ANOVA and regression-based interpretations and optimization efforts (Eze et al., 2025; Hundie, 2022).

3.4 Effect of Interaction between Process Variables on Mahogany Seed Oil Biodiesel Yield

The 3D response surface plot (Figure 5) effectively illustrates the significant interaction effect between reaction time (A) and temperature (B) on biodiesel yield, observed at a fixed methanol/oil ratio of 8:1 and catalyst concentration of 3 wt%. The visual evidence of a rising surface and non-parallel contour lines strongly confirms this interaction, aligning with established principles in response surface methodology (RSM) where such features indicate that the effect of one factor is dependent on the level of another (Montgomery & Cahyono, 2022). Within the tested ranges, biodiesel yield generally increases with both longer reaction times and higher temperatures, with peak yields

achieved when both factors are elevated. This suggests a synergistic relationship, consistent with findings by (Saad et al., 2023) who also demonstrated that reaction time and temperature often interact to enhance biodiesel yield. Furthermore, this trend is supported by general biodiesel production principles were increasing both reaction time and temperature typically improves transesterification efficiency up to an optimal point (Demirbas, 2009). While these findings suggest that maximizing yield at these specific methanol/oil and catalyst concentration levels requires the combined use of longer reaction times and higher temperatures, it's important to consider that further optimization beyond the current experimental ranges and practical limitations may be necessary.

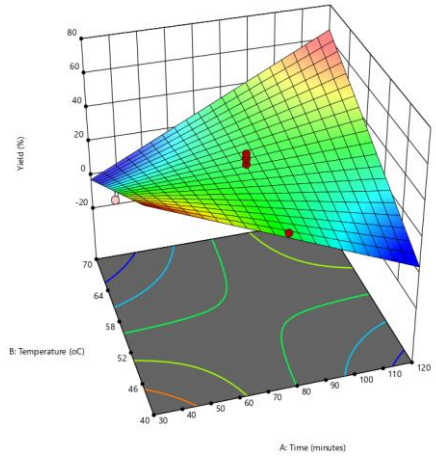

***Figure 5**: Interaction of Reaction Time and Temperature on Mahogany Seed Oil Biodiesel Yield*

The 3D surface plot (Figure 6) clearly illustrates the significant interaction between reaction time (A) and catalyst concentration (D) on biodiesel yield, maintaining a fixed temperature of 55°C and a methanol to oil ratio of 8:1. The curved surface and non-parallel contour lines visually confirm this crucial interaction. Within the experimental ranges, biodiesel yield consistently increases with both longer reaction times and higher catalyst concentrations, with the highest yields achieved when both parameters are elevated. This observed synergy aligns well with previous studies on biodiesel production optimization, where both reaction time and catalyst concentration have been shown to be critical, interacting synergistically to boost biodiesel yield (Bohlouli & Mahdavian, 2021; Hundie, 2022). Essentially, higher catalyst concentrations accelerate the transesterification reaction, while longer reaction times allow the process to approach completion, collectively leading to improved yields.

However, the shape of the surface suggests a potential plateau or slight decrease in yield at the very highest levels of both factors, indicating that excessively high levels may not be continuously beneficial and that an optimal balance may exist at or near the upper limits of the experimental space explored under these fixed temperature and methanol-to-oil ratio conditions. This underscores the need to optimize both reaction time and catalyst concentration together to achieve maximum biodiesel production.

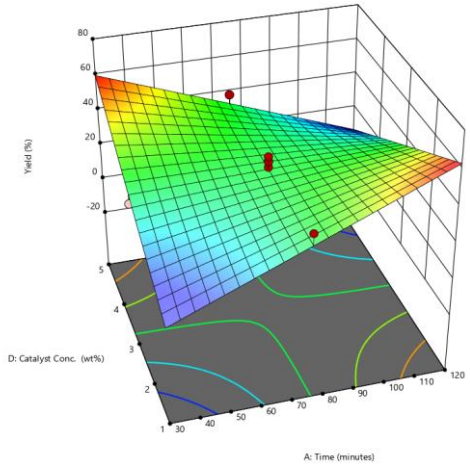

***Figure 6**: Interaction of Reaction Time and Catalyst Concentration.*

The 3D response surface plot (Figure 7) demonstrates a strong interaction between temperature (B) and the methanol/oil ratio (C), greatly impacting biodiesel yield. The steeply rising surfaces and non-parallel contour lines strongly confirm this interaction, a key indicator in response surface methodology, where both factors contribute to increased yield. This aligns with findings from (Chikhalikar et al., 2021), who observed optimal yields at elevated temperatures (around 80°C) and methanol/oil ratios near 7:1, emphasizing methanol's role in shifting reaction equilibrium. Similarly, (Mohamad et al., 2017) also reported consistent trends, achieving over 96.67% yield at 65°C and a 9:1 molar ratio, echoing our observed rising surface and interaction effects. These consistent findings confirm that the interaction between temperature and methanol/oil ratio is critical, with highest yields typically at the upper tested levels, though further optimization beyond current ranges should consider practical and economic constraints.

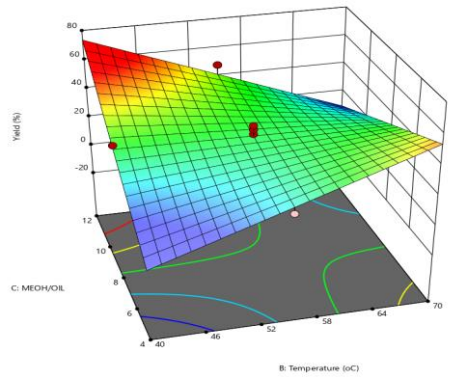

Figure 7: Interaction of Reaction Temperature and Methanol/oil Ratio.

The 3D response surface plot (Figure 8) illustrates a significant interaction between methanol/oil ratio (C) and catalyst concentration (D) on biodiesel yield. It shows yield peaks at higher methanol-to-oil ratios but, notably, at lower catalyst concentrations. This aligns with literature: HOSSAIN & MAZEN (2010) and Akhtar et al. (2023) reported that while higher methanol ratios boost yield, excessive catalyst can lead to reduced yields and saponification. Mansourpoor (2012) also found optimal yields with high methanol and moderate catalyst. These consistent findings emphasize the critical co-optimization of these parameters, as too much catalyst can be detrimental despite methanol's positive effect.

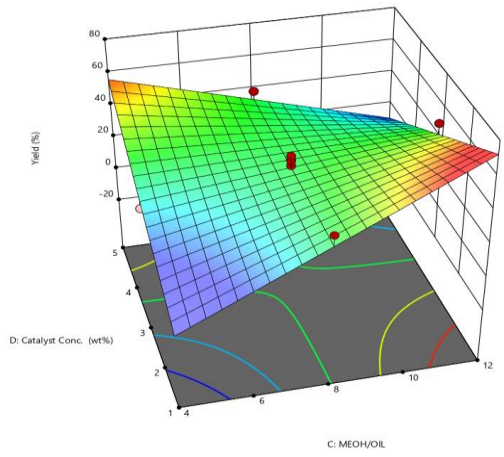

Figure 8: Interaction of Methanol/oil Ratio and Catalyst Concentration.

3.5 Optimization and Validation of Mahogany Seed Oil Biodiesel

Numerical optimization using the RSM model predicted a maximum biodiesel yield of 54.742% at the following optimal conditions: reaction time of 98 min, temperature of 63°C, methanol-to-oil molar ratio of 10:1, and catalyst concentration of 2 wt%, with a desirability of 93.3%. A validation experiment conducted under these optimized conditions resulted in an average biodiesel yield of 55.16%, which closely agrees with the predicted value, validating the model's predictive capability. These results are comparable to those reported by (Muhammad et al., 2023) and higher than those reported by (Arazo et al., 2016), considering the differences in feedstock, catalyst, and experimental setup.

3.6 Characterization of Calcined Banana Peel

To comprehensively characterize the prepared calcined banana peel catalyst, a suite of analytical techniques was employed. This section details the findings from Brunauer-Emmett-Teller (BET) analysis, Fourier Transform Infrared Spectroscopy (FTIR) and Scanning Electron Microscopy (SEM), providing insights into the catalyst's textural properties, elemental composition, and surface chemistry.

3.6.1 Brunauer-Emmett-Teller (BET) Analysis of Calcined Banana Peel

The textural properties of the calcined banana peel catalyst, as determined by BET characterization (Table 9), demonstrate its excellent structural features for catalytic applications. The catalyst exhibited a high BET surface area of 527.6 m^2/g, confirmed by a BJH surface area of 533.2 m^2/g, and a pore volume of 0.264 cm^3/g.

Table 9: BET Characterization of Calcined Banana Peel

S/N	Parameter	Value	Unit
1	Surface Area by BJH	533.2	m^2/g
2	Surface area by BET	527.6	m^2/g
3	Pore Volume (BJH)	0.264	cm^3/g
4	Pore Diameter (BJH)	2.125	nm
5	Micro pore Volume	0.186	cm^3/g
6	Micropore Surface area	522.05	m^2/g

Dubinin-Astakhov (DA) analysis (Figure 9) revealed a mesoporous structure with a dominant pore size centred around 3 nm. This is slightly comparable to the study of Madai et al. (2020) who reported a BET surface area of 411.2 m^2/g and a mesoporous structure with an average pore size of 3.014 nm for their calcined banana ash (CBA) catalyst, which was blended with Li-$CaO/Fe_2(SO_4)_3$. Notably, the catalyst in this study exhibits a significantly higher BET surface area (527.6

m²/g) compared to Madai's 411.2 m²/g, suggesting a greater availability of active sites.

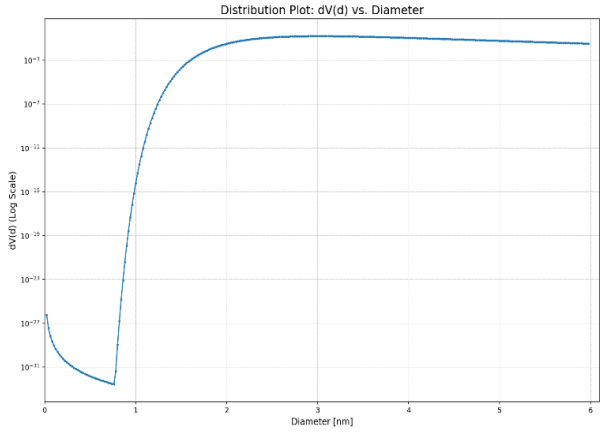

Figure 9: *Pore Size Distribution of the Calcined Banana Peel Catalyst*

Furthermore, the dominant pore size of approximately 3 nm in our catalyst is remarkably similar to the 3.014 nm reported in the study of Madai et al. (2020), both falling within the optimal mesoporous range for biodiesel transesterification. This pore size range (2-10 nm) is widely recognized as ideal for transesterification reactions, allowing efficient diffusion of triglyceride molecules while providing abundant active sites (Lee et al., 2014; Soltani et al., 2017). While Madai et al. (2020) utilized a more complex catalyst system involving blended metal compounds, the simply calcined banana peel catalyst in this study achieves superior surface area while maintaining comparable and favourable microporosity. This aligns with research by Daimary et al. (2022), who demonstrated that calcined agricultural wastes could develop highly accessible mesoporous structures rivalling synthetic catalysts. The textural superiority confirms that the straightforward calcination approach employed in this work is highly effective in generating a bio-based catalyst with excellent structural characteristics, potentially leading to enhanced catalytic performance for biodiesel production through improved mass transfer and reactant accessibility.

3.6.2 Characterization of Calcined Banana Peel Catalyst by SEM-EDS

To clarify the textural features and elemental composition of the calcined banana peel catalyst, Scanning Electron Microscopy and Energy Dispersive X-ray Spectroscopy (SEM-EDS) characterization was conducted. Figure 8 illustrates the SEM micrographs (a–c) at progressively higher magnifications and the corresponding EDS elemental analysis (d).

The SEM images (Figure 10a–c) reveal the hierarchical porous structure of the calcined material. At the lowest magnification (100 µm scale bar, Figure 10a), the catalyst exhibits a heterogeneous morphology composed of agglomerated particles with a rough, irregular surface texture. Notably, interparticle voids and intraparticle pores are evident, suggesting inherent porosity.

As magnification increases (80 µm, Figure 10b; 50 µm, Figure 10c), the porous network becomes more defined, closing in a sponge-like architecture at the highest resolution (Figure 10c). This interconnected framework, characterized by abundant mesopores and macropores, aligns with the high surface area (BET analysis) and pore volume reported earlier. The calcination process thus successfully transformed banana peel into a lightweight, macroporous scaffold, ideal for catalytic applications.

The EDS spectrum (Figure 10d) identifies the catalyst as a carbon-rich material (73.91 at%, 55.38 wt%) with significant potassium (9.62 at%, 23.46 wt%). The elevated carbon content likely stems from residual char or inorganic carbonates formed during calcination, while potassium—present as oxides or carbonates—serves as a potent solid base catalyst for transesterification reactions. Nitrogen (10.01 at%, 8.75 wt%) may originate from nitrogenous compounds in the banana peel, and calcium (1.15 at%, 2.87 wt%) reflects the mineral ash content. Trace elements (Si, Cl, Mg, P, Na, Al, S, Fe) account for ≤2.87 wt% collectively, with no detectable titanium.

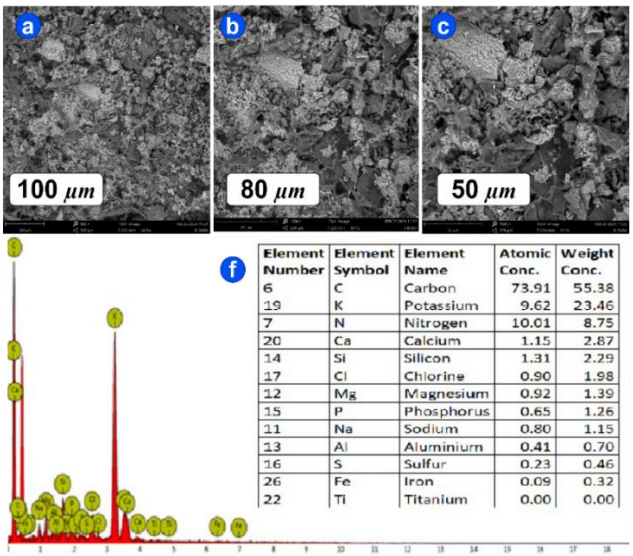

Figure 10: *SEM-EDS Characterization of Calcined Banana Peel Catalyst: (a-c) Micrographs Showing a Rough and Porous*

Surface Morphology; (d) EDS Spectrum and Elemental Composition Indicating a Carbon-Rich Material with Trace Amounts of Potassium and Other Elements

The EDS spectrum (Figure 10d) identifies the catalyst as a carbon-rich material (73.91 at%, 55.38 wt%) with significant potassium (9.62 at%, 23.46 wt%). The elevated carbon content likely stems from residual char or inorganic carbonates formed during calcination, while potassium—present as oxides or carbonates—serves as a potent solid base catalyst for transesterification reactions. Nitrogen (10.01 at%, 8.75 wt%) may originate from nitrogenous compounds in the banana peel, and calcium (1.15 at%, 2.87 wt%) reflects the mineral ash content. Trace elements (Si, Cl, Mg, P, Na, Al, S, Fe) account for ≤2.87 wt% collectively, with no detectable titanium.

The SEM-EDS data corroborate the exceptional textural and compositional attributes of the catalyst. The porous morphology (SEM) facilitates reactant diffusion and active site accessibility, while the potassium-enriched carbon matrix (EDS) enhances catalytic activity. These synergistic features position the calcined banana peel as a promising bio-based catalyst for sustainable biodiesel production, combining high surface area, favourable porosity, and intrinsic catalytic functionality.

3.6.3 Fourier Transform Infrared Spectroscopy (FTIR) analysis of Calcined Banana Peel

FTIR spectroscopy was utilized to investigate the chemical composition, and functional groups present in the calcined banana peel catalyst, offering insights into its potential catalytic behaviour. Figure 11 presents the transmittance FTIR spectrum of the material.

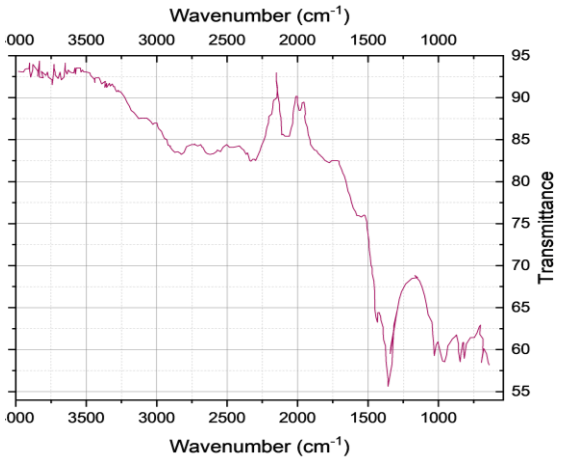

***Figure 11**: FTIR Spectrum of Calcined Banana Peel Catalyst.*

1. Hydroxyl Groups (O–H Stretching): A broad absorption band centred at 3400 cm^{-1} corresponds to O–H stretching vibrations, indicative of surface hydroxyl groups and adsorbed water. This aligns with prior studies on banana peel ash (Madai et al., 2020; Betiku et al. (2016)), which attributed similar bands (3424–3433 cm^{-1}) to hydroxyl functionalities, confirming the catalyst's hydrophilic nature.
2. Aliphatic Carbon–Hydrogen (C–H Stretching): A sharp peak at ~2920 cm^{-1} reflects trace residual aliphatic organic matter (e.g., cellulose-derived compounds), consistent with cocoa pod ash analyses (Ofori-Boateng & Lee, 2013). This suggests incomplete combustion during calcination, leaving minor carbonaceous residues.
3. Carbonate Ions (CO_3^{2-}): A prominent band at ~1440 cm^{-1} corresponds to asymmetric C–O stretching in carbonate ions, corroborating findings in CaO-based catalysts (Satapathy et al., 2023). This feature strongly implicates the presence of potassium carbonate (K_2CO_3), a known solid base catalyst for transesterification.
4. Metal–Oxygen (M–O) Vibrations: A broad, intense band below 1000 cm^{-1}, peaking at ~870 cm^{-1}, is attributed to M–O stretching in metal oxides (e.g., K_2O, CaO). This overlaps with reports in banana peel ash (Madai et al., 2020; Betiku et al., 2016) and underscores the catalyst's mixed oxide/carbonate framework. The overlapping O–C–O bending mode of carbonates in this region further supports the coexistence of these functional groups.

The FTIR data confirm the calcined banana peel catalyst's chemical heterogeneity, characterized by dominant basic carbonate species (e.g., K_2CO_3) and metal oxides (e.g., K_2O, CaO). These functional groups impart intrinsic basicity, critical for facilitating biodiesel transesterification through methanol deprotonation and triglyceride activation. Additionally, the persistence of hydroxyl groups (3400 cm^{-1}) and residual aliphatic organics (2920 cm^{-1}) suggests potential contributions to surface acidity or secondary active sites, which may enhance reaction efficiency. The integration of carbonate-derived basicity with metal oxide frameworks ensures both catalytic activity and structural stability, aligning with the porous morphology observed via SEM. These findings synergize with SEM-EDS results, underscoring the catalyst's dual functionality and reinforcing its viability

as a sustainable, multifunctional material for efficient biodiesel production.

3.7 Characterization of Optimum Mahogany Seed Oil Biodiesel

Following catalyst characterization, the produced mahogany biodiesel underwent comprehensive analysis to determine its fuel quality and suitability for use in diesel engines. This section details the evaluation of key physicochemical properties according to established ASTM standards, providing a robust assessment of the biodiesel's fuel characteristics.

3.7.1 Physicochemical Analysis of Optimum Mahogany Seed Oil Biodiesel

The analysis of physicochemical properties of mahogany biodiesel, presented in Table 10, demonstrates that it largely adheres to the ASTM D6751 standards for biodiesel fuel. Key fuel properties such as kinematic viscosity, flash point, heating value, and cetane number are well within or exceed the ASTM specifications, indicating good fuel quality and potential for efficient engine performance. The biodiesel also exhibits acceptable pour and cloud points for moderate climates. A primary deviation from the ASTM standard is the acid value, which is higher than the specified limit, suggesting a need for further optimization in production or refining to reduce acidity. Overall, the physicochemical properties of mahogany biodiesel are promising, indicating its potential as a viable biofuel, particularly with attention to reducing the acid value to meet ASTM D6751 standards fully.

Table 10: Physiochemical Properties of Mahogany

Parameters	Mahogany	ASTM- D6751
Density (g/cm^3)	0.855	0.86 to 0.9
Refractive index	1.551	-
Viscosity (mPas)	2.81	-
Kinematic viscosity (Cp)	3.29	1.9 to 6.0
Acid value (mg/g)	1.31835	0.5
Free fatty acid (ffa)	0.659175	-
Saponification value (mg/g)	159.885	≤370
Iodine value (mg/g)	80.2008	≤120
Peroxide value (meq/kg)	10.0	-
Flash point (°C)	125.3	100 to 170
Pour point (°C)	-1.9	-5 to 10
Cloud point (°C)	1.4	-5 to 17
Heating value (MJ/kg)	39.1201	≥ 35
Cetane number	62.3918559	≥ 51

FTIR Analysis of Optimum Mahogany Seed Oil Biodiesel

FTIR analysis of the mahogany biodiesel produced (Figure 12) confirmed its chemical identity as fatty acid methyl esters (FAMEs). The spectrum showed several key absorption bands characteristic of biodiesel (Mursiti et al., 2019). The most prominent feature was a sharp, intense peak at 1743 cm-¹, clearly attributed to the carbonyl (C=O) stretching vibration of ester groups (Arazo et al., 2016; Rosset & Perez-Lopez, 2019), a widely accepted primary indicator of ester linkages and successful biodiesel formation (Chukwuneke et al., 2016). Further confirming the FAME structure were strong bands in the 2800-3000 cm-¹ region, attributed to aliphatic C-H stretching vibrations of the fatty acid alkyl chains (Arazo et al., 2016; Hossain et al., 2021), and prominent C-O stretching bands in the 1000-1300 cm-¹ range, characteristic of ester C-O-C linkages (Chukwuneke et al. 2016), forming a recognized "ester fingerprint region" (Mursiti et al. 2019).

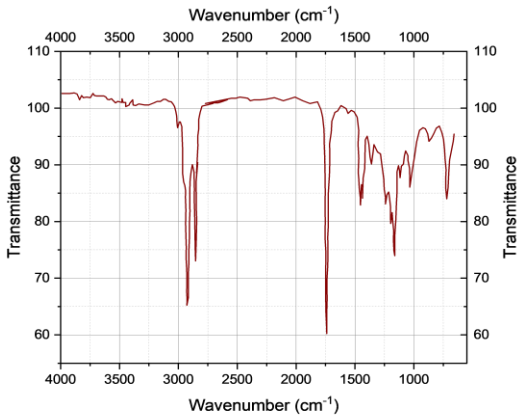

Figure 12: *Fourier Transform Infra-Red (FTIR) Spectra of Optimum Mahogany Seed Oil Biodiesel.*

In addition, the spectrum showed minimal intensity around 3400 cm-¹, indicating the absence of a significant broad O-H band. This suggests a low concentration of hydroxyl-containing impurities such as unreacted methanol, water, or residual free fatty acids and glycerol (Wembabazi et al., 2015), and is indicative of good biodiesel purity and effective removal of potential contaminants during production and purification (Arazo et al. 2016). In summary, FTIR analysis robustly confirms the successful transesterification of mahogany oil to biodiesel based on the presence of key ester functional group bands, alkyl chain signatures, and the absence of significant impurity indicators.

3.7.2 Gas Chromatography Mass Spectrometry (GC-MS) of Optimum Mahogany Seed Oil Biodiesel

The GC-MS analysis of mahogany seed oil biodiesel produced with calcined banana peel catalyst (Table 11) revealed a diverse FAME profile dominated by methyl oleate and methyl linoleate. Methyl oleate appeared at multiple retention times (17.88, 26.18, and 31.75 min) with abundances ranging from 2.79% to 10.73%, while methyl linoleate showed significant presence across four peaks (25.63, 33.82, 36.33, and 37.72 min) with abundances between 7.22% and 12.68%. Minor components included methyl palmitate, methyl stearate, and trace amounts of glycerin (0.31%) and oleic acid (0.45%), indicating efficient transesterification and minimal free fatty acid content.

These findings align well with published literature on non-edible oil-derived biodiesel. The predominance of methyl oleate and methyl linoleate mirrors compositions reported in Jatropha-based biodiesel (Singh, 2024), while the minor FAME components match profiles documented in studies of sunflower biodiesels and mahogany seed oil (Baba et al. 2024; Chukwuneke et al. 2016). The low glycerin content confirms efficient transesterification, consistent with quality parameters cited by Mohan et al. (2016) and Ponce et al. (2021). The presence of less common compounds like chloroethyl linoleate (2.05%) and methyl octadecadienol (9.60%) may indicate specific feedstock characteristics or processing conditions, as occasionally noted in broader biodiesel literature (Eiserbeck et al., 2012).

Table 11: *GC-MS Analysis of Optimum Mahogany Seed Oil Biodiesel*

PK	RT (min)	Abundance (%)	Library/ID	Common Name
1	9.2179	0.2401	1,2-Dichloroethylene	Vinylidene chloride
2	9.4485	0.3145	Glycerin	Glycerol
3	17.8819	8.2623	9-Octadecenoic acid, methyl ester, (E)-	Methyl oleate
4	23.0934	0.4691	Hexadecanoic acid (Z), methyl ester	Methyl palmitate
5	25.6317	7.2211	12-Octadecenoic acid (Z), methyl ester	Methyl linoleate
6	25.7569	3.0984	cis-7,cis-11-Hexadecanoic acid (Z), methyl ester	Methyl hexadecadienoate
7	26.1775	2.7893	9-Octadecenoic acid, methyl ester, (E)-	Methyl oleate
8	26.5381	0.832	Methyl stearate	Methyl stearate
9	27.606	9.5967	2-Methyl-Z,Z-3,13-octadecadienol	Methyl octadecadienol
10	29.9572	0.4469	Oleic Acid	Oleic acid
11	30.3149	0.3051	12-Octadecenoic acid (Z), methyl ester	Methyl linoleate
12	31.2732	2.0502	2-Chloroethyl linoleate	Chloroethyl linoleate
13	31.7534	10.7293	9-Octadecenoic acid, methyl ester, (E)-	Methyl oleate
14	33.8213	12.4902	12-Octadecenoic acid (Z), methyl ester	Methyl linoleate
15	34.113	0.5022	9,17-Octadecadienal, (Z)-	Octadecadienal
16	35.3706	15.5466	9,12-Octadecadienoic acid (Z,Z)-	Linoleic acid
17	36.3286	12.6763	12-Octadecenoic acid (Z), methyl ester	Methyl linoleate
18	37.7214	12.4297	12-Octadecenoic acid (Z), methyl ester	Methyl linoleate

4 CONCLUSIONS

This study successfully demonstrated calcined banana peel as a sustainable heterogeneous catalyst for mahogany seed oil (MSO) biodiesel production. Response Surface Methodology (RSM) effectively modelled the transesterification process, with the developed quadratic model showing excellent statistical validity (F-value = 12.00, $p < 0.0001$, $R^2 = 0.8205$). ANOVA identified methanol-to-oil ratio as the most influential factor, while significant interaction effects between process variables highlighted their complex interdependencies requiring simultaneous

optimization. Model-based optimization determined optimal conditions of 98 minutes reaction time, 63°C temperature, 10:1 methanol-to-oil ratio, and 2 wt% catalyst concentration, yielding a predicted 54.74% biodiesel production. Experimental validation achieved 55.16% yield, confirming excellent model reliability. Catalyst characterization revealed exceptional properties: high BET surface area (527.6 m^2/g), optimal mesoporous structure (3 nm pore size), and abundant active basic sites from K_2O, CaO, and carbonate species. These features ensure high catalytic activity and reusability potential. The produced biodiesel met most ASTM specifications with excellent cetane number (62.39), kinematic viscosity (3.29 cP), flash point (125.3°C), and heating value (39.12 MJ/kg). Only the acid value slightly exceeded standards, indicating need for minor process refinement. This study advances sustainable biodiesel technology by valorising two agricultural wastes (mahogany seeds and banana peels) within a circular economy framework. The findings demonstrate that waste-derived catalysts can enable economically viable, environmentally friendly biodiesel production, contributing significantly to renewable energy solutions and sustainable bioeconomy practices.

REFERENCES

Akhtar, R., Hamza, A., Razzaq, L., Hussain, F., Nawaz, S., Nawaz, U., Mukaddas, Z., Jauhar, T. A., Silitonga, A. S., & Saleel, C. A. (2023). Maximizing biodiesel yield of a non-edible chinaberry seed oil via microwave assisted transesterification process using response surface methodology and artificial neural network techniques. *Heliyon*, *9*(11), e22031. https://doi.org/10.1016/j.heliyon.2023.e22031

AOCS, A. O. C. S. (2017). *Peroxide Value - Acetic Acid-Chloroform Method (Official Method Cd 8-53)*. (7th edition, Official Methods and Recommended Practices of the AOCS). AOCS Press.

Arazo, R. O., Abonitalla, M., Gomez, J., Quimada, N., Yamuta, K., Mugot, D., & Hanif, P. (2016). BIODIESEL PRODUCTION FROM Swietenia macrophylla (MAHOGANY) SEEDS. *Journal of Higher Education Research Disciplines*, *1*(2), 8–18.

ASTM, A. I. (2021). *ASTM D1218-21: Standard Test Method for Refractive Index and Refractive Dispersion of Hydrocarbon Liquids* (ASTM International). ASTM International.

ASTM, I. (2018). Standard test method for acid number of petroleum products or lubricating oils (D664-18e2). *ASTM International*. https://doi.org/10.1520/D0664-18E02

Betiku, E., Akintunde, A. M., & Ojumu, T. V. (2016). Banana peels as a biobase catalyst for fatty acid methyl esters production using Napoleon's plume (Bauhinia monandra) seed oil: A process parameters optimization study. *Energy*, *103*, 797–806. https://doi.org/10.1016/j.energy.2016.02.138

Bohlouli, A., & Mahdavian, L. (2021). Catalysts used in biodiesel production: a review. *Biofuels*, *12*(8), 885–898. https://doi.org/10.1080/17597269.2018.1558836

Chikhalikar, M., Markapuram, S. R., Kamble, R., Tiwari, B., & Gidwani, K. (2021). Optimizing the Yield of Biodiesel Made from Waste Soybean Oil by Varying the Temperatures and Volumetric Ratios of Oil and Methanol. In P. V. Baredar, S. Tangellapalli, & C. S. Solanki (Eds.), *Advances in clean energy technologies: select proceedings of ICET 2020* (pp. 403–414). Springer Singapore. https://doi.org/10.1007/978-981-16-0235-1_32

Chukwuneke, J., Sinebe, J., Ugwuegbu, D., & Agulonu, C. (2016). Production by Pyrolysis and Analysis of Bio-oil from Mahogany Wood (Swietenia macrophylla). *British Journal of Applied Science & Technology*, *17*(4), 1–9. https://doi.org/10.9734/BJAST/2016/24551

Daimary, N., Boruah, P., Eldiehy, K. S. H., Pegu, T., Bardhan, P., Bora, U., Mandal, M., & Deka, D. (2022). Musa acuminata peel: A bioresource for bio-oil and by-product utilization as a sustainable source of renewable green catalyst for biodiesel production. *Renewable Energy*, *187*, 450–462. https://doi.org/10.1016/j.renene.2022.01.054

Degfie, T. A., Mamo, T. T., & Mekonnen, Y. S. (2019). Optimized Biodiesel Production from Waste Cooking Oil (WCO) using Calcium Oxide (CaO) Nano-catalyst. *Scientific Reports*, *9*(1), 18982. https://doi.org/10.1038/s41598-019-55403-4

Demirbas, A. (2009). Progress and recent trends in biodiesel fuels. *Energy Conversion and Management*, *50*(1), 14–34. https://doi.org/10.1016/j.enconman.2008.09.001

Eiserbeck, C., Nelson, R. K., Grice, K., Curiale, J., & Reddy, C. M. (2012). Comparison of GC–MS, GC–MRM-MS, and GC × GC to characterise higher plant biomarkers in Tertiary oils and rock extracts. *Geochimica et Cosmochimica Acta*, *87*, 299–322. https://doi.org/10.1016/j.gca.2012.03.033

Eze, S. O., Amamba, K. K., Jeremi, L. O., Aliyu, A., Ejikeme, C. S., Akoh, M. D., Adedapo, A. O., Abbas, A. O., Ibraheem, P. L., Hillary, G. E., Adisa, E. I., Idris, A., Ojinika, A. P., Iheanacho, B. C., John, S. O., & Jean Baptiste, M. A. (2025). Optimizing Biodiesel Yield and Fuel Properties from Waste Avocado Oil: A Comparative Study of RSM and ANFIS Learning Models. *Progress in Chemical and Biochemical Research*.

HOSSAIN, A. B. M. S., & MAZEN, M. A. (2010). Effects of catalyst types and concentrations on biodiesel production from waste soybean oil biomass as renewable energy and environmental recycling process. *Australian Journal of Crop Science*, 500–555.

Hossain, M., Goni, Muntaha, L. K. M. O., Jamal, N., Sujan, M. S., Ahmed, S., Islam, M. S., Bhuiyan, R. H., & Fakhruddin, A. N. M. (2021). Box-Behnken design-based optimization for biodiesel production from waste cooking oil using Mahogany (Swietenia macrophylla) fruit shell derived activated carbon as a heterogeneous base catalyst. *Reaction Kinetics, Mechanisms and Catalysis*.

Hundie, K. B. (2022). Optimization of Biodiesel Production Parameters from Cucurbita maxima Waste Oil Using Microwave Assisted via Box-Behnken Design Approach. *Journal of Chemistry*, *2022*, 1–12. https://doi.org/10.1155/2022/8516163

Jensen, W. A. (2014). Design and analysis of experiments by douglas montgomery: A supplement for using JMP®. *Journal of Quality Technology*, *46*(2), 181–181. https://doi.org/10.1080/00224065.2014.11917962

Lee, A. F., Bennett, J. A., Manayil, J. C., & Wilson, K. (2014). Heterogeneous catalysis for sustainable biodiesel production via esterification and transesterification. *Chemical Society Reviews*, *43*(22), 7887–7916. https://doi.org/10.1039/c4cs00189c

Mansourpoor, M. (2012). Optimization of Biodiesel Production from Sunflower Oil Using Response Surface Methodology. *Journal of Chemical Engineering & Process Technology*, *03*(05). https://doi.org/10.4172/2157-7048.1000141

Mohamad, M., Ngadi, N., Wong, S. L., Jusoh, M., & Yahya, N. Y. (2017). Prediction of biodiesel yield during transesterification process using response surface methodology. *Fuel*, *190*, 104–112.

Mohan, M. R., Jala, R. C. R., Kaki, S. S., Prasad, R. B. N., & Rao, B. V. S. K. (2016). Swietenia mahagoni seed oil: A new source for biodiesel production. *Industrial Crops and Products*, *90*, 28–31. https://doi.org/10.1016/j.indcrop.2016.06.010

Montgomery, D. C., & Cahyono, S. (2022). *Design and Analysis of Experiments, 9th Edition*.

Muhammad, K. M., Adeyemi, M. M., & Umoru, P. E. (2023). Optimization of Biodiesel Production from Seeds of Cotton and Calabash Via In Situ Transesterification using CaO as Catalyst. *Tropical Journal of Natural Product Research*, *7*(2), 2432–2436. https://doi.org/10.26538/tjnpr/v7i2.21

Mursiti, S., Fitriani Rahayu, E., Maylia Rosanti, Y., & Nurjaya, I. (2019). Mahogany seeds oil: isolation and characterizations. *IOP Conference Series: Materials Science and Engineering*, *509*, 012137. https://doi.org/10.1088/1757-899X/509/1/012137

Ofori-Boateng, C., & Lee, K. T. (2013). The potential of using cocoa pod husks as green solid base catalysts for the transesterification of soybean oil into biodiesel: Effects of biodiesel on engine performance. *Chemical Engineering Journal*, *220*, 395–401. https://doi.org/10.1016/j.cej.2013.01.046

Ponce, E. L. A., Ochoa-Herrera, V., Quintanilla, F., Egas, D. A., & Mora, J. R. (2021). Optimization of a gas chromatography methodology for biodiesel analysis. *Journal of Analytical Chemistry*, *76*(1), 106–111. https://doi.org/10.1134/S1061934821010093

Rosset, M., & Perez-Lopez, O. W. (2019). FTIR spectroscopy analysis for monitoring biodiesel production by heterogeneous catalyst. *Vibrational Spectroscopy*, *105*, 102990. https://doi.org/10.1016/j.vibspec.2019.102990

Saad, M., Siyo, B., & Alrakkad, H. (2023). Preparation and characterization of biodiesel from waste cooking oils using heterogeneous Catalyst(Cat.TS-7) based on natural zeolite. *Heliyon*, *9*(6), e15836. https://doi.org/10.1016/j.heliyon.2023.e15836

Singh, M. R. (2024). Utilization of mahogany seed oil as a renewable feedstock for cleaner biodiesel production. *Significances of Bioengineering & Biosciences*, *7*(1). https://doi.org/10.31031/SBB.2024.07.000653

Soltani, S., Rashid, U., Al-Resayes, S. I., & Nehdi, I. A. (2017). Mesoporous catalysts for biodiesel production. In *Clean energy for sustainable development* (pp. 487–506). Elsevier. https://doi.org/10.1016/B978-0-12-805423-9.00016-8

Wembabazi, E., Mugisha, P. J., Ratibu, A., Wendiro, D., Kyambadde, J., & Vuzi, P. C. (2015). Spectroscopic Analysis of Heterogeneous Biocatalysts for Biodiesel Production from Expired Sunflower Cooking Oil. *Journal of Spectroscopy*, *2015*, 1–8. https://doi.org/10.1155/2015/714396